



$\delta^{18}\text{O}$ and δD of streamwaters across the Himalaya and Tibetan Plateau: Implications for moisture sources and paleoelevation reconstructions

Michael T. Hren^{a,*}, Bodo Bookhagen^b, Peter M. Blisniuk^c, Amanda L. Booth^d, C. Page Chamberlain^e

^a Department of Geology & Geophysics, Yale University, 210 Whitney Ave. New Haven, CT 06511, United States

^b Department of Geography, University of California Santa Barbara, 1832 Ellison Hall, Santa Barbara, CA 93106-4060, United States

^c Department of Environmental Earth System Science, Stanford University, 450 Serra Mall, Braun Hall, Building 320, Stanford University, Stanford, CA 94305-2115, United States

^d Water and Environmental Research Center, Institute of Northern Engineering, University of Alaska, Fairbanks P.O. Box 755860, Fairbanks, Alaska 99775-5860, United States

^e Department of Environmental Earth System Science, Stanford University, 450 Serra Mall, Braun Hall, Building 320 Stanford University, Stanford, CA 94305, United States

ARTICLE INFO

Article history:

Received 22 May 2009

Received in revised form 6 August 2009

Accepted 25 August 2009

Editor: P. DeMenocal

Keywords:

paleoelevation
paleoaltimetry
Tibetan Plateau
Himalaya
isotopes
precipitation

ABSTRACT

This study presents new $\delta^{18}\text{O}$ and δD data from 191 streams across the Himalaya and Tibetan Plateau to better constrain the spatial variability of stable isotopes in modern precipitation over this region. Moisture penetrating into the southeastern Tibetan Plateau is predominantly derived from monsoonal airmasses originating from the Bay of Bengal and transported into the eastern Himalayan syntaxis along the Brahmaputra River. Progressive rainout during orographic lifting and cooling results in clear relationships between $\delta^{18}\text{O}$ and δD and catchment hypsometric elevation on the plateau margin. However, monsoonal-derived moisture is progressively mixed with central Asian airmasses in more western and northern parts of the Tibetan Plateau. As a result, predicted isotope–elevation relationships that are based on empirical lapse rates or thermodynamic models of the isotopic evolution of an airmass produce large (1–3 km) misfits between measured and predicted catchment elevations for much of the Tibetan Plateau, including some areas directly north of the central Himalayan crest. This suggests that changes in the $\delta^{18}\text{O}$ or δD of paleoprecipitation on the central and southwestern Tibetan Plateau may reflect surface uplift along moisture transport pathways or changes in the penetration of monsoonal-derived moisture rather than regional surface uplift histories.

© 2009 Elsevier B.V. All rights reserved.

1. Introduction

Stable-isotope paleoelevation reconstructions of the Tibetan Plateau rely on empirical data or model-based assumptions of the relationship between the $\Delta\delta^{18}\text{O}$ or $\Delta\delta\text{D}$ of precipitation and elevation that can be applied to paleoprecipitation isotope proxy localities (e.g. Garzione et al., 2000a; Rowley et al., 2001; Poage and Chamberlain, 2001). In recent years, a global network for isotopes in precipitation (GNIP) has been established by the International Atomic Energy Agency to monitor long-term patterns and changes in the $\delta^{18}\text{O}$ and δD of global precipitation and relationships with geographical parameters. While this network has provided valuable baseline data on the isotopic composition of global precipitation, large areas such as the Himalaya and Tibetan Plateau are characterized by a single isotope-monitoring station. Thus, paleoenvironmental interpretations of isotopic records in this region commonly rely on global (Bowen and Revenaugh, 2003) or regional (Liu et al., 2008a,b) models of the isotopic composition of precipitation that were derived from relatively few and distal sampling stations. Moreover, model predictions for $\delta^{18}\text{O}$ in high elevation areas

with complex moisture sources can deviate from actual site measurements by +5 to –5‰ (Liu et al., 2008a,b), a range that greatly exceeds the variability observed in many paleoisotopic records of Cenozoic change (e.g. Garzione et al., 2000b, 2004; Rowley and Currie, 2006).

A number of studies have specifically examined $\delta^{18}\text{O}$, and to a lesser extent δD , in precipitation and groundwaters from the Himalayan front (e.g. Aizen et al., 1996; Pande et al., 2000; Garzione et al., 2000a; Karim and Veizer, 2002), Tibetan Plateau (e.g. Wushiki, 1981; Yu and Zhang, 1981; Zhang, 1997; Zhang et al., 2002; Tian et al. 2001a, b, c, 2003; Quade et al., 2007), and Southeast Asia (Araguás-Araguás and Froehlich, 1998; Liu et al., 2008a,b) to identify the environmental and geographical controls of the isotopic composition of precipitation in this region. Data from the Himalayan front (Garzione et al., 2000a) and the eastern edge of the Tibetan Plateau (Yu and Zhang, 1981) show a clear relationship between the altitude of groundwater sampling sites and the measured $\delta^{18}\text{O}$ (–0.3‰/100 m elevation) that agrees with global isotope lapse data (Poage and Chamberlain, 2001) and model predictions for the distillation of an airmass during orographic ascent and progressive rainout (Rowley et al., 2001; Rowley, 2007; Rowley and Garzione, 2007). However, stable isotope measurements of precipitation (Tian et al., 2001a,b,c, 2005, 2007, 2008) and groundwaters at sites across the plateau (Yu and Zhang, 1981; Wushiki, 1981; Quade et al., 2007) show strong latitudinal controls on the $\delta^{18}\text{O}$ of water across this region.

* Corresponding author.

E-mail address: mhren@umich.edu (M.T. Hren).

Because of the lack of baseline precipitation isotope data for the Tibetan Plateau, isotopic relationships from waters collected on the Himalayan front or from models that are calibrated for the orographic lifting, cooling, and rainout of a single airmass have been used to interpret changes in isotopic records from across the Tibetan Plateau and its northern-bounding basins with respect to surface elevation change (e.g. Graham et al., 2005; Rowley and Currie, 2006; DeCelles et al., 2007; Reiser et al., 2008; Wang et al., 2008; Murphy et al., 2009; Saylor et al., 2009; Kent-Corson et al., 2009). Although the isotopic composition of precipitation is shown to be directly related to elevation on the Himalayan front (Garzzone et al., 2000a,b; Rowley et al., 2001), precipitation (Tian et al., 2001a, b, c) and groundwater (Quade et al., 2007) data show that $\delta^{18}\text{O}$ and δD values increase northward across the Tibetan plateau likely as a result of changes in the dominant source of moisture to different plateau regions (e.g. Tian et al., 2007; Quade et al., 2007). Importantly, the controls of isotopes of precipitation across the Tibetan Plateau and the impact of mixing of continental and monsoonally-derived moisture on predicted elevation and $\Delta\delta^{18}\text{O}_{\text{precip}}$ or $\Delta\delta\text{D}_{\text{precip}}$ relationships are unclear.

In the modern environment, the isotopic composition of precipitation provides a conservative tracer for the origin, phase transitions, and transport paths of water (Dansgaard, 1964; Rozanski et al., 1993; Gat, 1996). Variations in $^{18}\text{O}/^{16}\text{O}$ and D/H ratios of meteoric precipitation are dominantly controlled by atmospheric parameters such as temperature, relative humidity, and evaporation (Dansgaard, 1964; Yurtsever and Gat, 1981; Rozanski et al., 1993), and by geographic factors such as altitude, latitude, moisture source, and transport process (e.g. Craig, 1961; Siegenthaler and Oeschger, 1980; Gat, 1996; Kendall and Coplen, 2001; Karim and Veizer, 2002). Fundamentally, interpretations of the causes of past spatial variability or changes in the isotopic composition of precipitation rely on detailed understanding of the controls of spatial variability of modern isotopes of precipitation. Streamwaters can provide a time-integrated record of the isotopic composition of precipitation (Fritz, 1981; Gat, 1996; Kendall and Coplen, 2001) and thus a first-order measure of broad factors controlling regional-scale isotopes of precipitation.

We collected water from 191 streams during low-flow periods from several catchments in the eastern Himalaya and southern and central Tibetan Plateau to examine the environmental and atmospheric controls on the isotopic composition of groundwater, and thus precipitation. These data are compared with satellite measurements of seasonal precipitation, mean and precipitation-weighted basin elevations, and geographical parameters to examine the sources of moisture to the southern and central Tibetan Plateau and provide new constraints on the application of stable isotopic records of precipitation for paleoclimate and

paleoelevation reconstructions across this region. These data show a significant decrease in the transport of monsoonal moisture north and west of $\sim 30^\circ\text{N}$ and $\sim 86^\circ\text{E}$, and increased recycling of continental moisture and contributions from Central Asian airmasses with distance from the southeastern plateau margin. Southwestern and central Tibetan Plateau streams are characterized by inverse isotope–elevation relationships that could produce significant misestimates of paleoelevation.

2. Description of field area and sampling

The Himalaya are a 2000 km long east–west trending mountain belt that significantly shapes the climate of Southeast Asia and the northern Hemisphere (Clemens et al., 1991). On the southern front of the range, precipitation patterns are dominantly controlled by the Indian Summer Monsoon (ISM) circulation (Bookhagen et al., 2005; Anders et al., 2006; Bookhagen and Burbank, 2006). During the summer period, moisture is transported from the Bay of Bengal and Southeast Asia northwest along the range front where it is orographically lifted and adiabatically cooled producing heavy monsoonal rainfall. On the eastern edge of the range, moisture penetrates the Himalaya along the Siang–Brahmaputra river valley bringing seasonal monsoonal moisture fluxes to the southern Tibetan Plateau. Mean annual precipitation across the Himalaya and Tibetan Plateau ranges from greater than 3 m/yr south of the Himalaya along tributaries of the Siang to less than 0.2 m/yr in central and western Tibet (Domroes and Peng, 1988; Bookhagen and Burbank, 2006). The contribution of summer precipitation (May to Oct) to the annual total ranges from $\sim 80\%$ south of the range to greater than 95% in the uppermost reaches of the Brahmaputra and central Tibetan Plateau. Traditionally, the maximum northward transport of summer monsoonal moisture was thought to extend as far north as the Tanggula Mountains ($\sim 33^\circ\text{N}$) which separate the southern Tibetan Plateau from the Qinghai province. However, there is considerable uncertainty over the relative contributions of southern-derived moisture from the Bay of Bengal and recycled precipitation carried to the Tibetan Plateau across Eurasia by the regional westerlies (Tian et al., 2001a,b,c, 2005, 2007, 2008).

We sampled small tributaries of the Brahmaputra, Sutlej, Siang, and other major drainages across the Tibetan Plateau, High Himalaya, and Himalayan front (Fig. 1; Supplement) between 1998 and 2006 to examine the controls of the isotopic composition of groundwaters. Water samples from small drainages are grouped by the major rivers that they flow into including the Nyang Tsangpo, Lower, Middle, and Upper Yarlung Tsangpo, Po Tsangpo, Siang Tsangpo, and a number of small tributaries in the Southern and Central Tibetan Plateau.

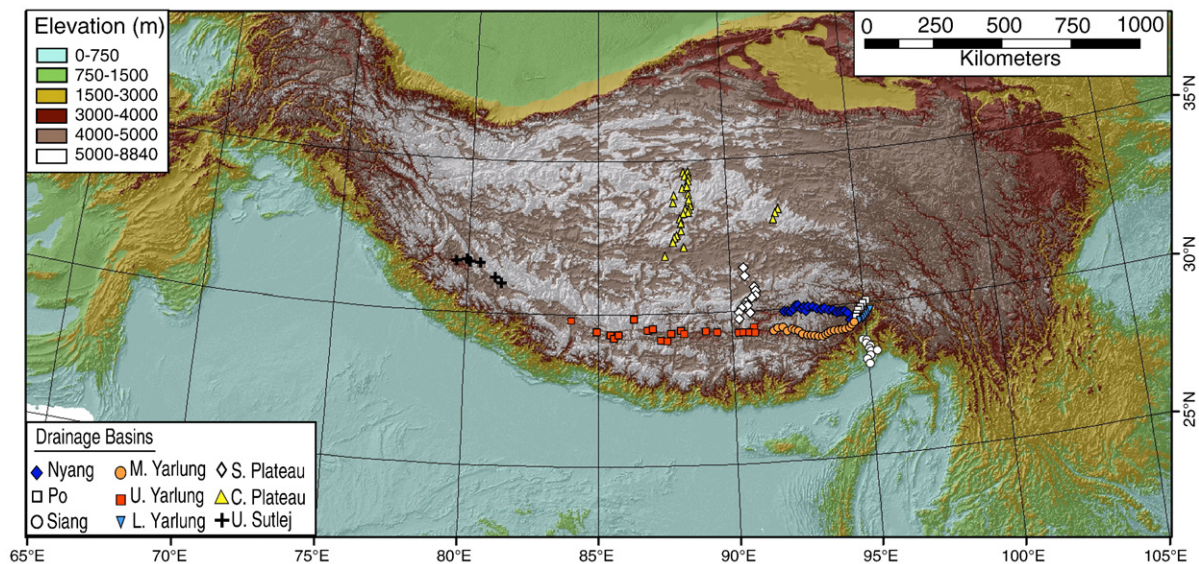


Fig. 1. Sample location map of stream waters from across the Himalaya and Tibetan Plateau.

Sample collection sites range from 278 m south of the Himalaya to 5205 m elevation in the Central Tibetan Plateau region. Snowline in the southern Tibetan Plateau region ranges from 4500 to 4700 m, however the lower extent of most glaciers along the Brahmaputra is ~5000–5200 m. Sampled drainage basin sizes range from <1 km² to ~5800 km², with the majority of sampling localities from basins <250 km² (Appendix A Table 1). Basin mean and precipitation-weighted basin elevation was quantified using a patched 90 m Shuttle Radar Topography Mission (SRTM V2) digital elevation model. Seasonal rainfall amounts are derived from calibrated Tropical Rainfall Measurement Mission (TRMM) satellite measurements averaged over 8 years (Bookhagen and Burbank, 2006). Due to the small size of the bulk of catchments analyzed, catchment mean elevation is nearly identical to precipitation-weighted basin elevation within the resolution of DEM and satellite data (Appendix A). In areas with steep terrain, the uncertainty introduced by DEM and rainfall–satellite resolution results in greater misfit between precipitation-weighted and basin-mean elevation. Discrepancies between precipitation-weighted catchment elevation and basin mean elevation are most apparent for streams in the high-relief, deeply incised eastern syntaxis region. However inclusion of these catchments in evaluation of the data does not in any way impact our conclusions.

Samples were filtered through 0.45 μm nylon filters and collected in 60 mL HDPE bottles. Samples along the middle and lower portions of the Brahmaputra were collected during low-flow periods before the summer monsoon in May 2004 and April 2005. Samples south of the Himalaya from tributaries of the Siang Tsangpo were collected in February 2006. Samples from the upper reaches of the Brahmaputra and southern Tibetan Plateau were collected in August/September 2005 and September 2006, while samples from the central Tibetan Plateau area were sampled in August 1998 and May/June 1999. Although some samples from the upper Brahmaputra and central Tibetan Plateau were collected during the summer monsoon periods, in both localities more than 95% of precipitation to these areas was contributed during this period and these samples were collected after peak monsoonal precipitation. Moreover, rainfall in these areas is less than 0.2 m/yr and samples most likely reflect flow from groundwater and snowmelt, not recent rain events. Thus, any possible impact of recent precipitation events prior to water collection are negligible, as this water likely reflects the dominant seasonal precipitation.

3. Analytical methods

The water samples collected in central Tibet during 1998 and 1999 were analyzed during a pilot study in 2000. The oxygen isotope measurements were made using a Prism II mass spectrometer and hydrogen isotope measurements were made on a SIRA 12 mass spectrometer by zinc reduction (Vennemann and O'Neil, 1993). The results were scaled to correct for instrumental biases between laboratories and isotope compositions are reported relative to VSMOW (Gonfiantini, 1978). Water samples from 2004 to 2006 were analyzed for δ¹⁸O in duplicate by CO₂–H₂O gas equilibration (Epstein and Mayeda, 1953) in continuous flow using a GasBench attached to a ThermoFinnigan Delta Plus XL. δD of groundwaters were measured in triplicate by H₂ reduction of water using a Thermal Conversion Elemental Analyzer in continuous flow and attached to a ThermoFinnigan Delta Plus XL. Analytical precision (2σ) was better than ±0.2‰ and 2‰ for δ¹⁸O and δD respectively. The isotopic composition of Tibetan and Himalayan groundwaters are reported in per mil (‰) relative to VSMOW (Gonfiantini, 1978).

4. δ¹⁸O and δD of precipitation

Measured δ¹⁸O_{water} ranged from –6.2‰ south of the Himalaya to –20.8‰ in the high-elevation headwaters of the Brahmaputra. δD_{water} ranged from –33‰ to –165‰ at these same localities (Appendix A Table 1). Two samples from lakes in the central Tibetan Plateau were characterized by extremely enriched isotopic compositions of –4‰ and –43 for δ¹⁸O and δD, respectively. In general, isotope data fall closely

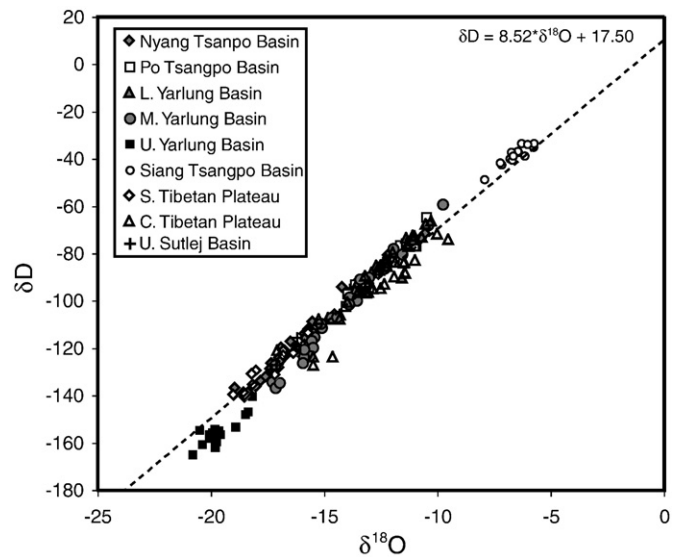


Fig. 2. δ¹⁸O and δD values of stream waters across the Tibetan Plateau. Samples are categorized with respect to the larger catchment they drain. Isotopic compositions fall closely about the GMWL, however local MWL vary between the large catchments studied.

about the global meteoric water line calculated from GNIP sites where δD = 8.17 * δ¹⁸O + 10.35. Regression of all data show a steeper Himalayan and Tibetan Plateau river meteoric water line of δD = 8.52 * δ¹⁸O + 17.50 (Fig. 2), which is consistent with the MWL for the High Himalaya with a slope of 8.7 and intercept of 29.9 (Pande et al., 2000). Examination of data from individual catchments or segments of the Brahmaputra, Siang, and Tibetan Plateau reveal large differences in localized river meteoric water lines (Appendix A Table 2) that possibly reflect local evaporation of soil or groundwaters. Streams along the highest reaches of the Brahmaputra, the middle and upper Yarlung basins, exhibit the steepest local river meteoric water lines (slope of ~10 and intercept of ~38). Steep LMWL in these areas likely indicate evaporation in the high elevation portions of the drainages, which are also characterized by the least precipitation along the Brahmaputra and extensive evaporite mineral inputs to river waters (Hren et al., 2007). LMWL in the southern and central Tibetan Plateau streams sampled have shallower slopes (7.3–8.1) that more closely reflect the GMWL. Tributaries of the Siang Tsangpo produce a LMWL with the lowest slope (6.4).

Total precipitation in the Himalaya and Tibetan Plateau decreases dramatically with increasing distance west from the eastern Himalayan syntaxis and with increasing distance north from the Himalayan range. Summer monsoon precipitation decreases from >1 m south of the range, to <0.1 m across much of the Tibetan Plateau with little variability in total rainfall across much of the high elevation landscape (Fig. 3A, B). The most negative δ¹⁸O and δD values are found in the upper reaches of the Brahmaputra, where nearly all moisture is derived from the summer monsoon. Areas with greater contribution of winter moisture (>5%), including areas south of the Himalaya and in the central plateau, are characterized by more positive δ¹⁸O and δD values (Fig. 4).

5. Spatial patterns of δ¹⁸O and δD values

Measured δ¹⁸O_{water} and δD_{water} show clear relationships with both latitude and longitude. Isotopic compositions become progressively depleted from south to north across the high Himalaya and along the course of the Brahmaputra (Figs. 5 and 6). However, north of 30°N latitude, δ¹⁸O and δD increase with increasing distance from the crest. For sites at elevations greater than 4 km and north of ~30°N, the relationship between latitude and δ¹⁸O_{water} is 1.75‰/°Latitude (R² = 0.74) and 15.7‰/°Latitude (R² = 0.72) for δD. δ¹⁸O values increase by ~8‰ from the southern Tibetan Plateau to the northernmost samples in the central Tibetan Plateau, south of the Altyn Tagh fault and the Tarim basin (Fig. 7).

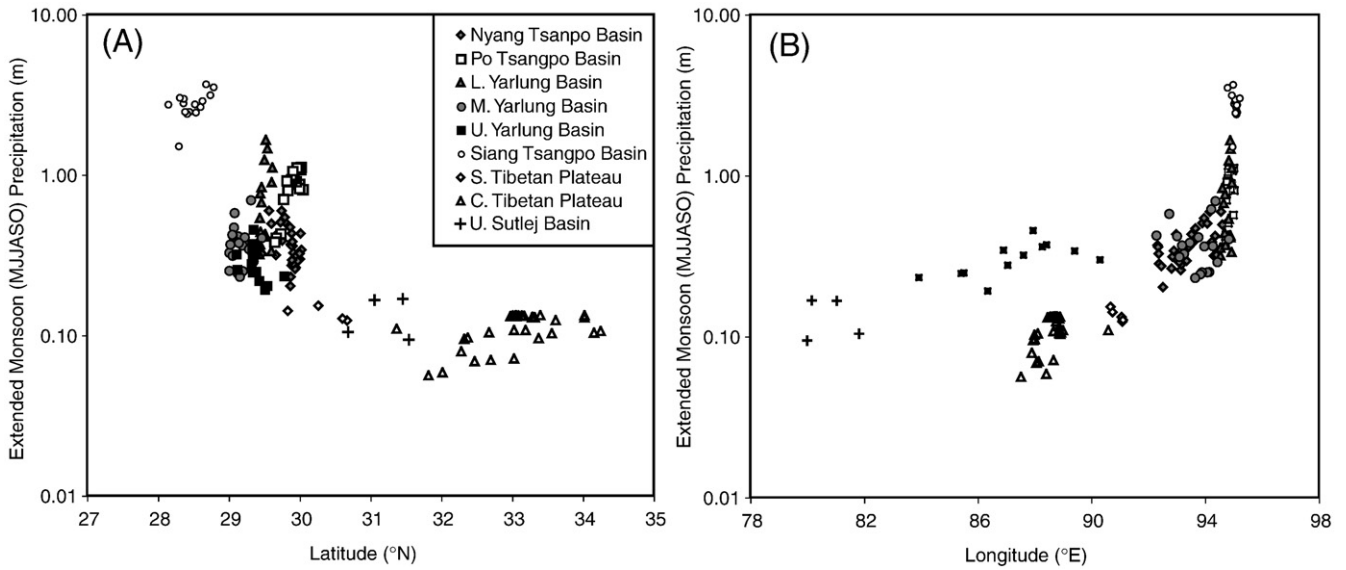


Fig. 3. Total precipitation during the extended summer monsoon period that ranges from May to Oct. as a function of latitude (A) and longitude (B). Summer monsoonal precipitation decreases significantly with increasing distance west along the Brahmaputra catchment and north from the Himalayan crest.

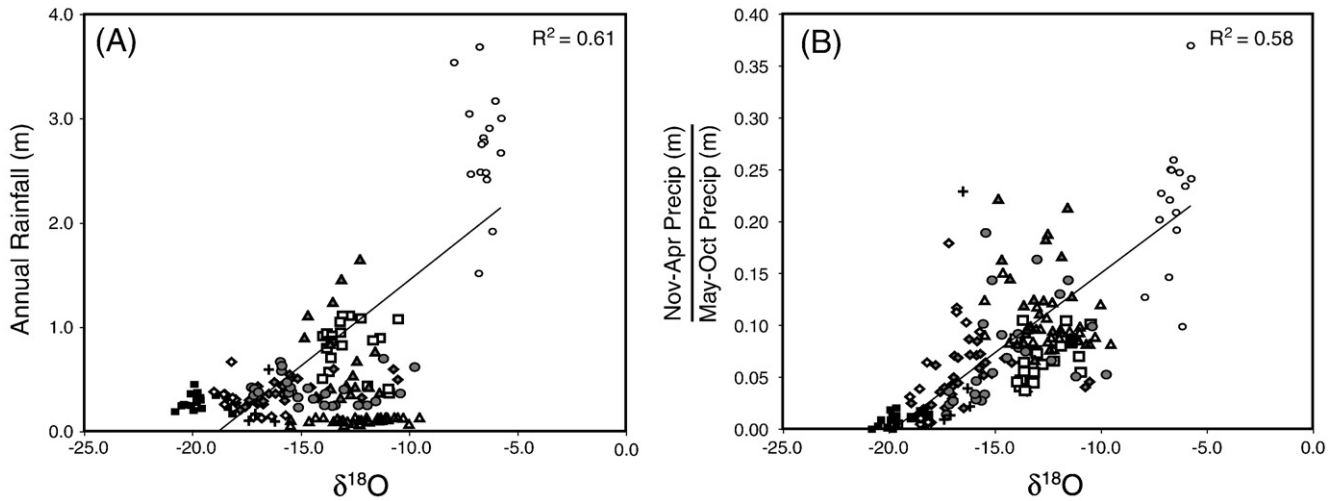


Fig. 4. $\delta^{18}\text{O}$ of streamwaters as a function total annual precipitation (A) and proportion of winter precipitation (B). Best-fit lines do not include streams from the Central Tibetan plateau.

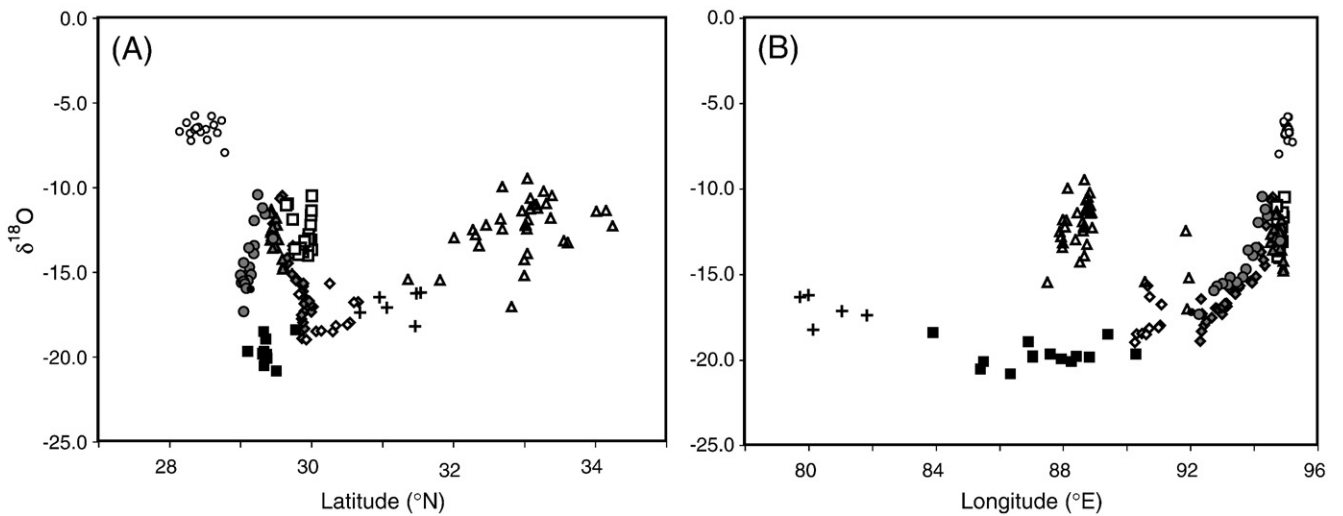


Fig. 5. $\delta^{18}\text{O}$ of streamwaters as a function of latitude (A) and longitude (B). Isotopic compositions become progressively more negative with increasing distance west and north from the eastern Himalayan syntaxis and reach a minimum at $\sim 30^\circ\text{N}$ and 86°E . West and north of these areas, progressive contributions of recycled and western-derived airmasses results in increasingly positive isotope values.

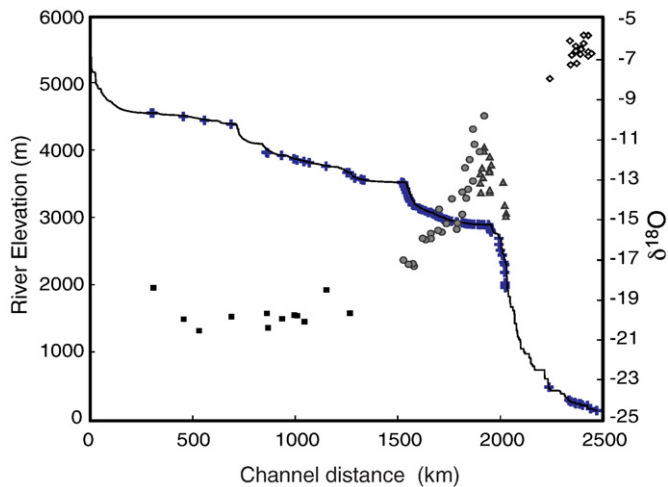


Fig. 6. Elevation profile of the Brahmaputra River and $\delta^{18}\text{O}$ of tributary waters along the downstream length.

$\delta^{18}\text{O}$ and δD values also decrease from east to west along much of the length of the Brahmaputra, and reach a minimum near $\sim 86^\circ\text{E}$. The major change in measured stream isotope values corresponds to changes in the elevation of stream sampling sites (Fig. 5B). However, west of $\sim 86^\circ\text{E}$ longitude, isotope values increase by a total of $\sim 6\text{‰}$ in $\delta^{18}\text{O}$ and $\sim 50\text{‰}$ in δD . This increase is coincident with the drainage divide between the Brahmaputra and Sutlej rivers near $\sim 82^\circ\text{E}$ longitude. Moreover, the headwaters of the Sutlej, which have higher mean and precipitation-weighted elevations than headwater tributaries of the Brahmaputra River, have higher $\delta^{18}\text{O}$ and δD values. $\delta^{18}\text{O}$ or δD values of waters from the Central Tibetan Plateau are offset from more southerly catchments of the Brahmaputra, Siang, and Southern Tibetan Plateau (south of 30°N latitude) and show little variation with longitude.

$\delta^{18}\text{O}$ and δD values from tributaries of the Brahmaputra and Siang show a strong correlation with the total annual precipitation ($R^2 = 0.61$), as well as the proportion of precipitation received during the Winter (November to April) monsoon ($R^2 = 0.58$). Sites that receive the largest proportion of the total yearly precipitation during the extended Summer monsoon period (May–Oct) show the lowest $\delta^{18}\text{O}$ values. Sites with greater contributions from winter moisture are characterized by a greater spread and generally more positive $\delta^{18}\text{O}$ or δD values.

6. Spatial patterns of deuterium-excess

The deuterium excess was defined by Dansgaard (1964) as $d = \delta\text{D} - 8 * \delta^{18}\text{O}$ and has values close to $+10\text{‰}$ for precipitation in temperate climates. Deuterium excess depends on relative humidity of an airmass at its oceanic origin, ocean surface temperature, and kinetic isotope effects during evaporation (Merlivat and Jouzel, 1979; Gat and Matsui, 1991; Koster et al., 1993; Kendall and Coplen, 2001), including the relative proportion of summer or winter precipitation that contributes to total precipitation amounts.

Deuterium excess values of stream waters decrease with progressive distance west (decreasing longitude) from ~ 15 to as low as -7 , with minimal relation to latitude. Similarly, d values are directly related to the mean basin elevation of streams analyzed with waters from mean basin elevations below 4 km characterized by d values above $+10\text{‰}$, while basins with elevations above 4 km have a wide range of values from $+15$ to -7‰ . These values fall well within the range of measured d in precipitation at Shiquanhe near the headwaters of the Sutlej River, and at Lhasa (Tian et al., 2007).

7. $\delta^{18}\text{O}$, δD and hypsometric basin elevation

Oxygen and hydrogen isotopes of streamwaters were compared against modern basin parameters (e.g., catchment mean elevation, relief, precipitation-weighted basin elevation) and empirical and theoretical predictions for $\Delta\delta^{18}\text{O}_{\text{precipitation}}$ and $\Delta\delta\text{D}_{\text{precipitation}}$ as a function of elevation. These were examined to assess the reliability of proxies that record the isotopic composition of paleo-precipitation and groundwater as an indicator of changes in paleoelevation. $\delta^{18}\text{O}$ or δD of waters from tributaries of the middle and lower Brahmaputra and Siang Tsangpo are strongly related to precipitation-weighted and basin-mean elevation. On average, $\delta^{18}\text{O}$ decreases by $\sim 0.29\text{‰}$ per 100 m hypsometric basin elevation change, a value similar to empirical data for the Himalayan front (Garzzone et al., 2000a,b) and a global calibration (Poage and Chamberlain, 2001). Isotope–catchment elevation data were also compared against predicted $\Delta\delta^{18}\text{O}$ of precipitation as a function of elevation using a thermodynamic model for the isotopic evolution of precipitation from an airmass during orographic ascent (e.g. Rowley et al., 2001; Rowley, 2007) with starting sea-level temperatures of 22°C , relative humidity of 85%, and $\delta^{18}\text{O}_{\text{precip}}$ of -3.6‰ , conditions similar to those found at Guwahati south of the eastern Himalayan front during the extended summer monsoon period (Fig. 8). Predicted isotope–elevation relationships from the thermodynamic model

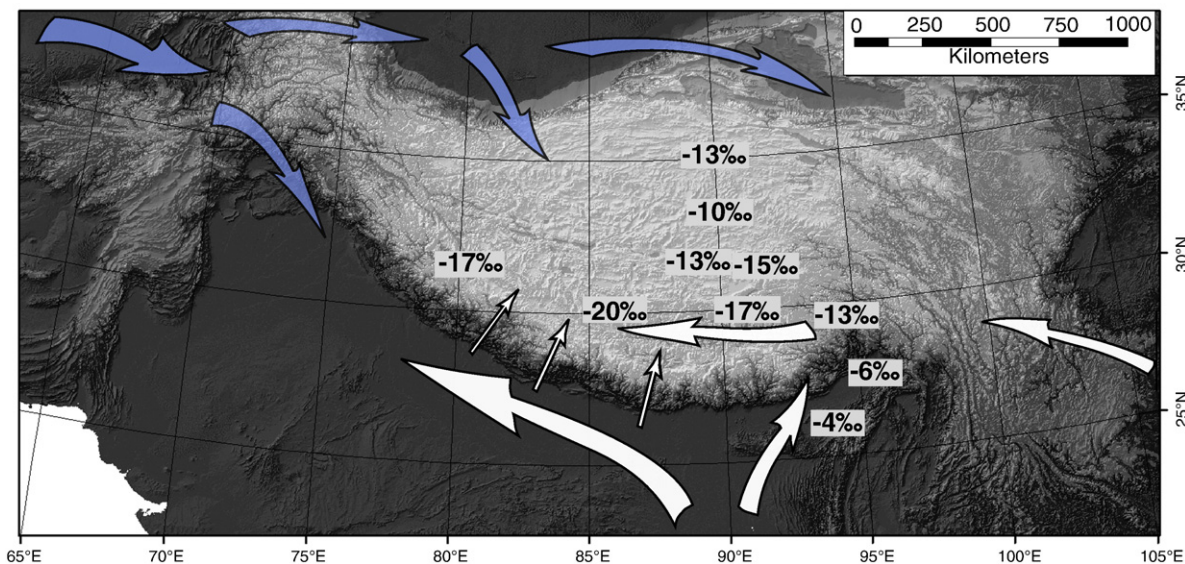


Fig. 7. Moisture transport pathways to the Himalaya and Tibetan Plateau and average stream $\delta^{18}\text{O}$ values. White arrows indicate Summer Monsoon moisture sources and blue arrows indicate (winter) westerly sources. Moisture along the Brahmaputra drainage is transported from the Bay of Bengal during the monsoon season into the southern Tibetan Plateau where it is progressively mixed with western-derived airmasses.

closely match (within 200 m) the empirical polynomial fit for stream waters from the Kali Gandaki drainage for a given change in $\delta^{18}\text{O}$ (Garzzone et al., 2000a,b). The majority of sites at low elevations and in the southern Tibetan Plateau fall closely about the polynomial empirical and model predictions for $\Delta\delta^{18}\text{O}$ as a function of elevation. However, streams from the central Tibetan Plateau are poorly represented by empirical or thermodynamic models for elevation– $\Delta\delta^{18}\text{O}$ relationships. Instead, these show a range of more than 12‰ in $\delta^{18}\text{O}$ and 70‰ in δD for sites with mean elevations higher than 4 km.

8. Discussion

8.1. Groundwater as a record of $\delta^{18}\text{O}$ and δD of precipitation

The isotopic composition of precipitation provides a record of the moisture sources and transport paths of an airmass. Over the course of a year, $\delta^{18}\text{O}_{\text{precipitation}}$ on the plateau can vary significantly (Tian et al., 2003), and GNIP isotope data show variations of more than 15‰ for $\delta^{18}\text{O}$ of precipitation at Lhasa throughout the year. Streamwaters record a time and precipitation-weighted signal of changing moisture sources and conditions during condensation. Water in streams is derived from groundwater, snowmelt, or recent precipitation that contributes to streamflow through overland or shallow subsurface flow. Depending on the recent hydrologic conditions and the physical setting of the stream catchment, the relative contributions of these components can vary, but in general the isotopic composition of groundwater closely reflects the weighted average annual isotopic composition of precipitation (Friedman et al., 1964; Yurtsever and Gat, 1981; Yonge et al., 1989). Indeed, measured $\delta^{18}\text{O}$ of streams near Lhasa ($\sim 17\text{‰}$) are nearly identical to weighted $\delta^{18}\text{O}_{\text{precipitation}}$ over 6 years at Lhasa meteorological station (Tian et al., 2003). Similarly, $\delta^{18}\text{O}_{\text{groundwater}}$ at the same latitude ($\sim 34^\circ\text{N}$) as Tuotuohe Meteorological station are within 1‰ (11–13‰ $\delta^{18}\text{O}$) of weighted $\delta^{18}\text{O}_{\text{precipitation}}$ values at this site (-11.95‰) (Tian et al., 2003), attesting to the utility of streamwater sampling as a record of annual weighted precipitation.

8.2. Moisture sources

Annual precipitation in the High Himalaya and southern Tibetan Plateau is dominated by the Indian Summer Monsoon (ISM), which

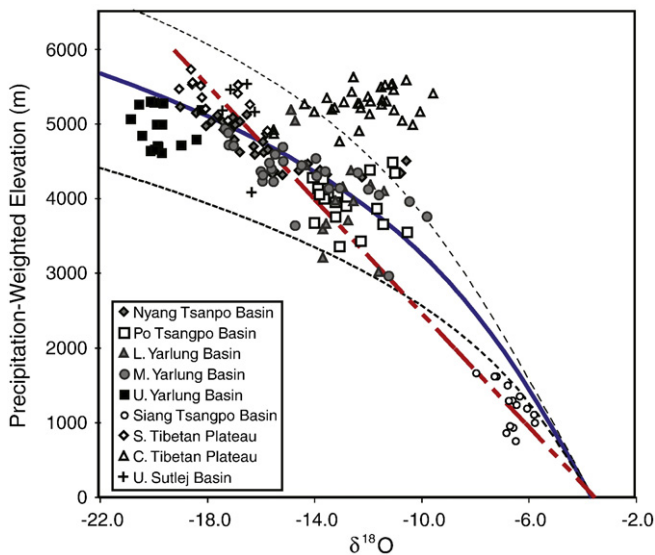


Fig. 8. $\delta^{18}\text{O}$ as a function of precipitation-weighted basin elevation. Predicted $\Delta\delta^{18}\text{O}$ for a starting $\delta^{18}\text{O} = -3.6\text{‰}$ using a simple linear (0.29‰/100 m; long dashed line) and a thermodynamic model output (solid line, dashed lines represent 95% confidence intervals; after Rowley, 2007; Rowley et al., 2001) with starting conditions similar to low elevations areas south of the eastern syntaxis region (22 °C, 85% RH) are shown.

develops in response to the movement of the InterTropical Convergence Zone (ITCZ) that separates wind circulation of the northern and southern hemispheres (Gadgil, 2003). Throughout the year, the ITCZ migrates north and south in response to changes in the sun's declination with a maximum summer extent of $\sim 33\text{--}35^\circ\text{N}$ (Araguás-Araguás and Froehlich, 1998). Latent heat released during condensation across the high elevation Tibetan Plateau amplifies warming of the central Asian landmass relative to surrounding oceans, driving the establishment of ISM air circulation patterns (Gadgil, 2003; Bookhagen et al., 2005; Bookhagen and Burbank, 2006).

In the eastern Himalaya, the development of temperature and pressure gradients related to the ITCZ pulls moisture from Southeast Asia and the Bay of Bengal and transports it northwestward. Precipitation measurements derived from passive microwave analysis show significant penetration of moisture along major river valleys into the orogen (Bookhagen et al. 2005) and around the eastern syntaxis and into the Southern Tibetan Plateau. The northward transport of water vapor is accompanied by increased evaporation of ambient precipitation, recycling of precipitated water, and mixing of waters carried across Eurasia or from the northwest corner of the Himalaya (Fig. 9).

$\delta^{18}\text{O}$ and δD values of streamwaters in the Himalaya and Tibetan Plateau provide support for satellite measures of the degree of penetration of southerly-derived moisture into the plateau. South of the Himalayan front and along the Brahmaputra river on the northern edge of the high Himalaya, the dominant control of the $\delta^{18}\text{O}$ and δD of streamwaters and thus precipitation is progressive distillation of airmasses during orographic ascent, cooling, and rainout. This is evidenced by a clear relationship between the isotopic composition of groundwater and the mean and precipitation-weighted basin elevations for streams south of the Himalaya and on the lower reaches of the Brahmaputra. Importantly, this relationship indicates a relatively narrow moisture source area in the Bay of Bengal and a simple transport path.

Deuterium excess (d) provides a measure of non-equilibrium isotope effects (Dansgaard, 1964) because it records the difference between the actual δD and expected equilibrium value based on measured $\delta^{18}\text{O}$. Deuterium excess is controlled by environmental conditions in the water–vapor source area, including relative humidity, temperature and wind speed over the evaporating surface, and the degree of water vapor recycling that occurs along the transport path of an airmass (Rozanski et al., 1993; Clark and Fritz, 1997). Under conditions of low humidity, strong kinetic isotope fractionation during evaporation produces high d values in subsequent precipitation (>10). Conversely, evaporation of moisture under conditions of high humidity results in decreased kinetic isotope fractionation, and subsequent precipitation derived from this moisture will have low d values ($<10\text{‰}$) (Dansgaard, 1964; Merlivat and Jouzel, 1979). Other processes such as partial evaporation of raindrops as they fall under conditions of low relative humidity, weak rainfall events, and higher temperatures can reduce d values measured in ground-level precipitation (Gat and Matsui, 1991; Gat, 1996; Araguás-Araguás et al., 1998).

Deuterium excess of waters south of the range and near the eastern Himalayan syntaxis are close to the global meteoric water value of $+10$, and consistent with moisture derived over a humid ocean. With increasing distance westward along the north edge of the Himalayan range, d values decrease in concert with $\delta^{18}\text{O}$ and δD to a minimum near 86°E longitude. As airmasses are transported into the interior of the Tibetan Plateau along the Brahmaputra catchment and are orographically lifted to >4 km elevation, progressive cooling, rainout, and distillation of moist airmasses result in clear isotope–elevation relationships. As airmasses travel farther to the interior during the summer monsoon, the total amount of southerly-derived moisture decreases, and the amount of recycled continental moisture increases. In the western Himalaya, rainfall distributions are

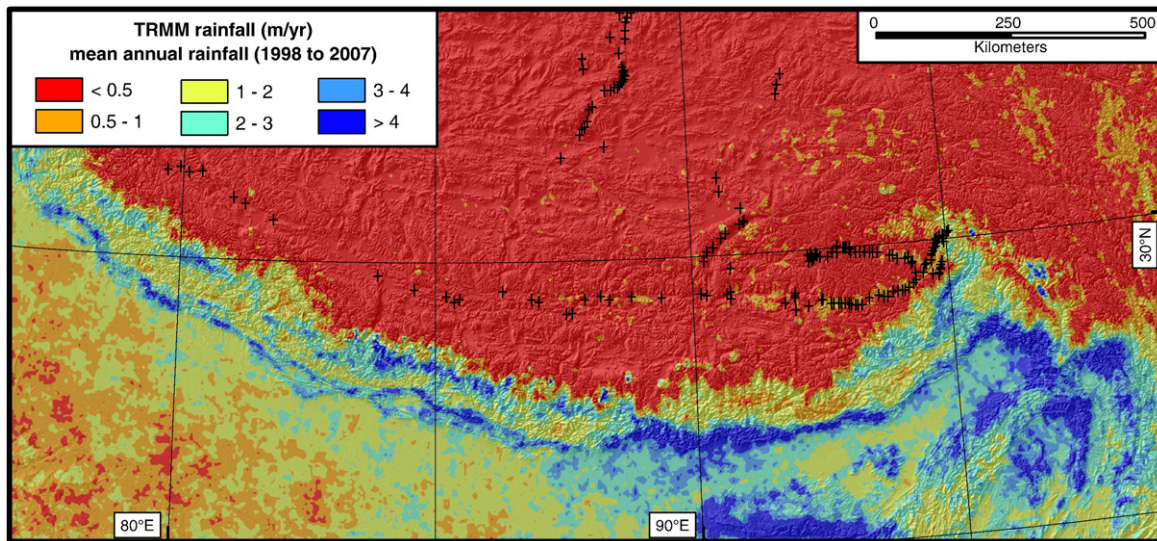


Fig. 9. TRMM satellite precipitation data for the Brahmaputra catchment calibrated after Bookhagen and Burbank (2006). Monsoonal moisture penetrates the southern Tibetan Plateau around the eastern Himalayan syntaxis and is carried westward along the Brahmaputra drainage and into the central Plateau.

controlled by both monsoonal moisture from Southeast Asia and the prevailing westerly winds (Lang and Barros, 2004; Bookhagen et al., 2005a; Dimri, 2006).

Summer monsoonal precipitation in the southern and western Tibetan plateau is characterized by low $\delta^{18}\text{O}$ and δD and d values relative to winter precipitation (Tian et al., 2007). This may be due, in part, to the high humidity of the moisture source area in the Indian Ocean and progressive distillation of moisture along the transport path. Areas of the Upper Brahmaputra River drainage and Central plateau only receive summer moisture from strong monsoonal activity, which is accompanied by low d values. Minimum d values occur in tributaries of the Upper Yarlung Tsangpo/Brahmaputra near 85° – 87°E longitude, indicating that summer monsoon moisture dominates groundwater recharge in this area of the plateau. $\delta^{18}\text{O}$, δD , and deuterium excess suggest the maximum westward extent of significant moisture transport from the eastern edge of the Himalaya lies in this range between 85° and 87°E longitude. Farther to the west, penetration of both summer rainfall sourced in the Bay of Bengal and winter westerly precipitation is dramatically reduced, but the proportion of moisture transported by the prevailing westerlies becomes more significant (Karim and Veizer, 2002). Recycled continental moisture produces higher d values, and greater contribution of westerly-derived airmasses and recycled moisture results in an inflection in groundwater isotope data near this longitude. This pattern of isotopic change is indicative of decreased moisture transport across the plateau, and is clearly evident in our calibrated, satellite-derived precipitation data (Fig. 9).

North of the Brahmaputra river drainage and the High Himalaya, isotopic compositions become progressively more negative to $\sim 30^{\circ}\text{N}$. North of this, $\delta^{18}\text{O}_{\text{water}}$ and $\delta\text{D}_{\text{water}}$ values become progressively more positive, despite constant elevations above 4 km, and d values range from -7 to 16% . This provides clear indication of changes to the dominant moisture sources to the central plateau and the decreasing role of the ISM to contributing moisture (Fig. 3). Constant summer precipitation and increasing $\delta^{18}\text{O}$ and δD values in streamwaters reflect decreasing contributions of southerly-derived moisture in areas where Central Asian climate is controlled by year-round westerlies and recycled moisture. While it is possible that single-season sampling could bias observed spatial patterns, replicate sample of several localities (Appendix A Table 1) shows minor variation between years and numerous studies show that groundwater reflects annual precipitation-weighted isotopic compositions.

8.3. Isotopes of groundwater and implications for paleoenvironmental reconstruction

Modern patterns of the isotopic composition of precipitation provide the basis for reconstructions of timing of major surface uplift of the Tibetan Plateau, intensification of the Indian Summer Monsoon, and long-term changes in regional paleoclimate (e.g. Thompson et al., 2000; Graham et al., 2005; Rowley and Currie, 2006; DeCelles et al., 2007; Reiser et al., 2008; Wang et al., 2008; Murphy et al., 2009; Kent-Corson et al., 2009). One of the earliest studies of isotopic composition of groundwaters across Tibetan Plateau (Yu and Zhang, 1981) provided clear evidence for a strong “altitude” effect on the $\delta^{18}\text{O}$ of precipitation of $\sim 0.3\%$ /100 m elevation at the edge of the Xizang plateau. More recent studies have confirmed this “altitude” effect in the Himalayan front (Garzzone et al., 2000a,b; Rowley et al., 2001).

Paleoclimatic or paleoelevation reconstructions rely on assumptions of the isotopic composition of precipitation at a given site, or predictable $\Delta\delta^{18}\text{O}$ or $\Delta\delta\text{D}$ –elevation relationships such as those observed on the range front. The hypsometric elevation of a catchment can be calculated from the measured $\Delta\delta^{18}\text{O}$ or $\Delta\delta\text{D}$ of groundwaters using empirical isotope–elevation lapse rates (Garzzone et al., 2000a,b; Poage and Chamberlain, 2001) or thermodynamic Rayleigh–distillation elevation–isotope models (Rowley et al., 2001, Rowley, 2007). We calculated the predicted basin elevation for individual catchments using measured stream $\delta^{18}\text{O}$ to evaluate how isotopic data reflect real basin parameters across the Himalaya and Tibetan Plateau. The purpose of this is not to calibrate isotope–elevation models, but rather to examine the broad characteristics of whether or not isotope paleoaltimetry approaches reasonably reproduce actual modern site elevations across the broad spatial scale of the Tibetan Plateau. Results show that at low elevations (< 4 km) and in the southernmost portion of the Tibetan Plateau, a Rayleigh isotope–elevation model, which produces predicted isotope–elevation relationships similar to a polynomial fit of southern Himalayan stream data (Garzzone et al., 2000a,b), reasonably reproduces basin elevations within ± 500 m of actual mean basin elevations for $\sim 75\%$ of streams analyzed. Nearly all sites with larger misfits are from tributaries with precipitation-weighted elevations higher than 4000 m (Fig. 10). However, in the central plateau and western portion of the Brahmaputra basin, inverse isotope–elevation relationships result in misfits between predicted and real hypsometric elevations. Specifically, although isotope measurements of streams from the upper Brahmaputra and

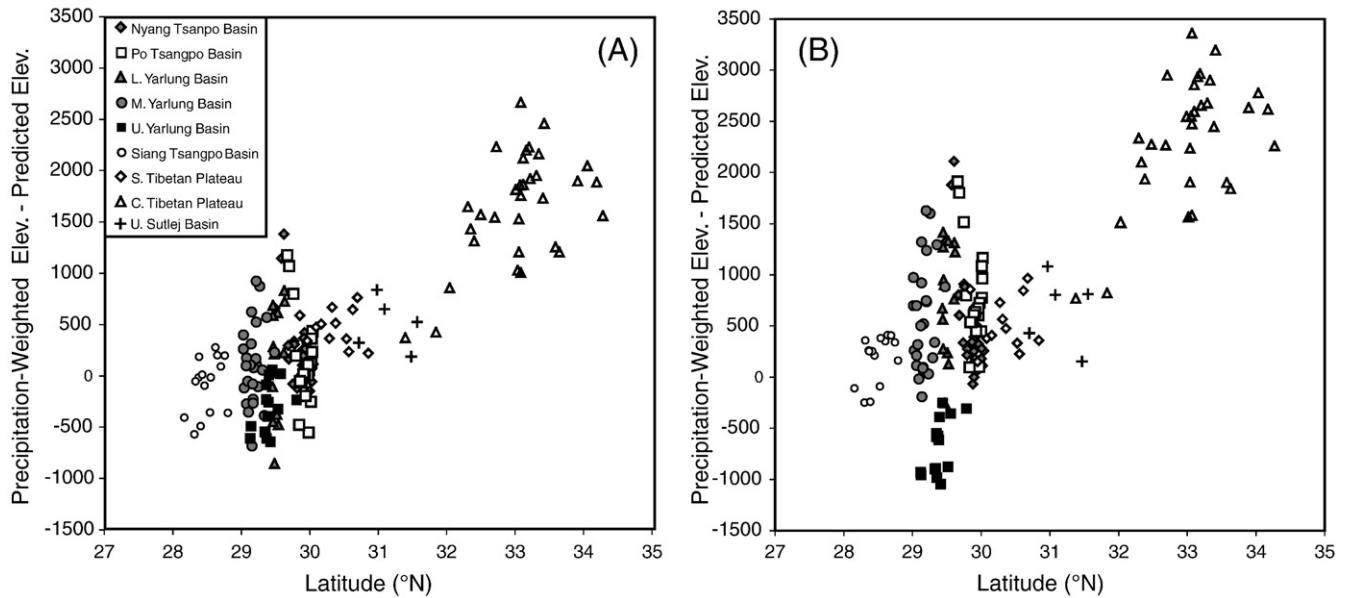


Fig. 10. Misfit between modern catchment precipitation-weighted elevation and the elevation predicted using calculated $\Delta\delta^{18}\text{O}$ as a function of elevation from a thermodynamic Rayleigh-distillation model shown in Fig. 9 (A) and an empirical linear isotope–elevation lapse rate (B).

Sutlej basins produce elevation estimates within ± 600 m of actual precipitation-weighted elevation, upper Brahmaputra streams produce underestimates of elevation while streams from the other side of the drainage divide in the U. Sutlej tributaries produce overestimates resulting in discrepancies of more than 1 km between similar elevation sites. More importantly however, streams from the central Tibetan Plateau show the largest misfit between model calculated elevation and actual basin elevations and consistently under predict site elevations by more than 1–3 km. This pattern results from the dramatic decrease in the percentage of southern-derived moisture with increasing distance from the Himalaya. Greater contributions of Central Asian, western-derived, and recycled moisture produces more positive groundwater $\delta^{18}\text{O}$ or δD values in northern plateau regions (north of $\sim 30^\circ\text{N}$) and along the southwestern Tibetan Plateau (west of $\sim 86^\circ\text{E}$). Application of simple Rayleigh distillation models to interpretations of oxygen or hydrogen isotope records from proxies for the isotopic composition of paleoprecipitation (i.e., $\delta^{18}\text{O}$ or δD of authigenic minerals or organic compounds) would significantly under predict past elevations for these regions (Fig. 10A). Moreover, application of a simple linear elevation–isotope model produces greater misfits between predicted elevations and precipitation-weighted elevation (Fig. 10B), with only 41% of all sites except Central plateau localities within ± 500 m of actual precipitation-weighted basin elevations and 70% within ± 800 m. Elevation estimates based on linear isotope lapse rates produce misfits of > 1500 m for nearly all Central Plateau sites. Importantly however, few data points fall significantly below the predicted empirical or modeled isotope–elevation relationships. This important result suggests that proxies that record low δD and $\delta^{18}\text{O}$ values of ancient precipitation clearly reflect high paleoelevations.

Long-term changes in the $\delta^{18}\text{O}$ or δD of authigenic minerals or organic compounds from many areas of the southwestern and central Tibetan Plateau may in fact reflect changes in the degree of penetration of moisture from the Bay of Bengal along the Brahmaputra rather than changes in local surface elevation. These changes to moisture transport could result from regional surface uplift, but could also reflect long-term global climatic changes. Varying intensity of the ISM and resultant changes in moisture transport into the plateau could produce changes in the isotopic composition of precipitation that could be interpreted as local surface uplift or downdrop (Vuille et

al., 2005; Blisniuk and Stern, 2005). Thus, interpretations of long-term $\delta^{18}\text{O}$ or δD records from sites across the Tibetan Plateau must consider modern patterns of isotopes of precipitation when evaluating long-term paleoclimatic or paleoenvironmental change.

9. Conclusions

We measured $\delta^{18}\text{O}$ and δD of 191 groundwaters from small catchments across the Himalaya and Tibetan Plateau to examine moisture sources to this region and further establish baseline isotope maps for paleoenvironmental reconstruction. While samples collected here reflect a narrow temporal period, to first order they provide an indication of the broad controls of modern stable isotopes of precipitation across the Tibetan Plateau. These data show that moisture in the southern Tibetan Plateau east of $\sim 86^\circ$ longitude is dominantly derived from airmasses originating over Southeast Asia and the Bay of Bengal and transported along the Brahmaputra river drainage. Airmasses penetrate the plateau through the eastern syntaxis of the Himalaya where they are orographically lifted and adiabatically cooled. Progressive rainout results in isotope–elevation relationships that are consistent with global empirical data and thermodynamic models for the isotopic evolution of precipitation in mountainous regions. These relationships hold, in the modern sense, as far north as $\sim 30^\circ\text{N}$ and as far west as 86°E . However, with increasing distance north and west across the plateau, increasing contributions of Central Asian and western-sourced airmasses results in progressively enriched isotopic signatures. This mixing of moisture sources produces misfits of 1–3 km between actual and predicted catchment hypsometric elevations for sites in the central Tibetan Plateau. Long-term changes in proxy records for the isotopic composition of paleoprecipitation for these regions may reflect changes in the position of the ITCZ and the Indian Summer Monsoon and resultant changes in the penetration of monsoonal moisture rather than local paleoelevation change.

Acknowledgements

The authors thank Libby Stern, Malinda Kent-Corson and Jacob Waldbauer for assistance collecting water samples in the field. The manuscript was improved through helpful comments and suggestions from C. Garzzone and an anonymous reviewer.

Appendix A

Table 1

Sample localities, basin parameters, and stream data.

Sample	Date sampled	Latitude	Longitude	Sample elevation (m)	Drainage area (km ²)	Basin Mean elevation (m)	Precipitation-weighted elevation (m)	Summer (MJJASO) rainfall (m/yr)	Winter (NDJFMA) rainfall (m/yr)	$\delta^{18}\text{O}$	δD	D-excess	Predicted hypsometric elevation ^a	Predicted hypsometric elevation ^b
<i>Nyang Basin Tributaries</i>														
05-Tibet-2	Apr 05	29.87445	92.32785	4639	27	5217	5221	0.37	0.01	-18.9	-137	15	5119	5290
05-Tibet-4	Apr 05	29.90062	92.34953	4527	5	5110	5115	0.36	0.01	-16.5	-117	14	4696	4438
05-Tibet-5	Apr 05	29.91348	92.36583	4450	156	5144	5139	0.33	0.01	-18.4	-139	8	5027	5089
05-Tibet-6	Apr 05	29.90897	92.38217	4428	32	4925	4917	0.29	0.01	-17.3	-127	12	4854	4735
05-Tibet-9	Apr 05	29.89078	92.45798	4296	63	4968	4963	0.27	0.01	-18.0	-136	8	4967	4963
05-Tibet-10	Apr 05	29.87252	92.52285	4220	21	5023	5027	0.19	0.01	-17.8	-134	8	4933	4893
05-Tibet-11	Apr 05	29.87368	92.68475	3982	751	5137	5105	0.22	0.01	-17.6	-132	8	4894	4816
05-Tibet-12	Apr 05	29.94425	92.81818	3824	335	5101	5081	0.26	0.01	-17.0	-128	8	4793	4618
05-Tibet-13	Apr 05	29.95573	92.85802	3780	60	4950	4950	0.30	0.01	-17.0	-127	9	4799	4630
05-Tibet-14	Apr 05	30.02948	92.90072	3673	321	4915	4902	0.33	0.01	-17.1	-126	11	4808	4647
05-Tibet-15	Apr 05	30.00522	93.01662	3600	152	5078	5026	0.29	0.01	-17.4	-129	10	4859	4746
05-Tibet-16	Apr 05	29.93442	93.14983	3500	75	5070	5025	0.25	0.01	-16.7	-121	13	4745	4528
05-Tibet-17	Apr 05	29.91100	93.17228	3462	146	5029	4979	0.25	0.02	-16.9	-120	15	4775	4584
05-Tibet-18	Apr 05	30.01297	92.98663	3624	18	4726	4728	0.42	0.02	-17.0	-124	12	4791	4615
05-Tibet-19	Apr 05	29.99957	93.03855	3645	34	4838	4778	0.30	0.02	-16.9	-126	10	4782	4598
05-Tibet-20	Apr 05	29.97577	93.10333	3568	8	4586	4617	0.27	0.02	-16.7	-124	10	4745	4528
05-Tibet-21	Apr 05	29.88862	93.25473	3420	64	4765	4753	0.32	0.02	-15.9	-114	13	4577	4229
05-Tibet-22	Apr 05	29.89158	93.35127	3371	1607	4912	4863	0.27	0.02	-15.7	-115	11	4552	4186
05-Tibet-23	Apr 05	29.88893	93.43667	3333	133	4577	4586	0.33	0.02	-16.2	-120	10	4637	4333
05-Tibet-24	Apr 05	29.89042	93.52512	3300	63	4624	4613	0.38	0.03	-15.8	-116	11	4571	4219
05-Tibet-25	Apr 05	29.89787	93.57210	3273	42	4652	4650	0.34	0.02	-15.7	-112	14	4541	4168
05-Tibet-26	Apr 05	29.86447	93.66765	3224	4188	4655	4694	0.41	0.04	-16.2	-120	9	4646	4350
05-Tibet-27	Apr 05	29.79427	93.90507	3150	87	4392	4360	0.47	0.03	-15.4	-114	10	4490	4084
05-Tibet-28	Apr 05	29.79248	93.96035	3138	69	4376	4323	0.52	0.03	-15.5	-109	15	4505	4108
05-Tibet-29	Apr 05	29.73373	94.07632	3148	160	4339	4314	0.47	0.02	-15.1	-111	10	4425	3978
05-Tibet-30	Apr 05	29.74732	94.16780	3116	34	4365	4315	0.58	0.02	-13.5	-92	16	4033	3407
05-Tibet-32	Apr 05	29.75545	94.23907	3070	172	4396	4377	0.35	0.02	-13.7	-96	14	4097	3494
05-Tibet-33	Apr 05	29.67757	94.35458	3004	302	4442	4371	0.39	0.03	-14.5	-106	10	4289	3769
05-Tibet-36	Apr 05	29.66615	94.31020	3136	232	4502	4458	0.29	0.02	-14.2	-94	19	4212	3655
05-Tibet-59	Apr 05	29.60170	94.60675	4155	32	4498	4495	0.47	0.02	-10.5	-72	13	3122	2387
05-Tibet-60	Apr 05	29.56785	94.56587	3508	20	4335	4333	0.57	0.02	-10.7	-74	12	3194	2455
05-Tibet-61	Apr 05	29.46985	94.39838	2964	308	4326	4280	0.29	0.02	-12.2	-81	17	3671	2959
<i>Po Tsangpo Basin Tributaries</i>														
05-Tibet-35	Apr 05	30.04112	95.01255	2030	86	3722	3557	0.68	0.08	-	-65	-	-	-
05-Tibet-37	Apr 05	30.02013	94.99733	2150	21	3719	3458	0.95	0.10	-	-72	-	-	-
05-Tibet-38	Apr 05	30.00893	94.97443	2183	2792	4320	2705	0.48	0.05	-13.7	-95	15	4089	3483
05-Tibet-39	Apr 05	30.00892	94.95777	2228	7	3695	3548	0.91	0.09	-10.5	-65	19	3115	2379
05-Tibet-40	Apr 05	29.99693	94.92385	2350	14	3922	3866	0.74	0.08	-11.6	-76	17	3506	2776
05-Tibet-41	Apr 05	30.00337	94.89647	2408	7	3682	3657	0.80	0.07	-11.4	-76	16	3424	2688
05-Tibet-42	Apr 05	29.99482	94.88112	2408	36	4104	4057	0.75	0.06	-13.1	-90	14	3930	3274
05-Tibet-43	Apr 05	29.98655	94.87257	2426	4	3428	3430	1.02	0.07	-12.2	-83	14	3685	2976
05-Tibet-44	Apr 05	29.96173	94.84702	2481	10	3945	3897	1.04	0.06	-12.8	-88	14	3843	3165
05-Tibet-45	Apr 05	29.95605	94.81378	2522	2	3371	3357	1.02	0.07	-13.0	-94	10	3913	3252
05-Tibet-46	Apr 05	29.94835	94.80262	2510	427	4061	4075	0.82	0.05	-13.6	-96	13	4073	3462
05-Tibet-47	Apr 05	29.94905	94.80317	2508	1695	4330	4278	0.44	0.04	-14.0	-102	10	4172	3599
05-Tibet-49	Apr 05	29.73275	94.72688	3324	178	4396	4384	0.38	0.03	-11.9	-82	14	3585	2862
05-Tibet-50	Apr 05	29.91095	94.79727	2697	6	3782	3754	0.88	0.07	-13.2	-91	14	3951	3301
05-Tibet-51	Apr 05	29.89988	94.79007	2730	3	3970	3950	1.00	0.04	-13.2	-94	11	3957	3309
05-Tibet-52	Apr 05	29.88137	94.78438	2851	21	4223	4136	0.89	0.04	-13.8	-96	14	4120	3526
05-Tibet-53	Apr 05	29.84662	94.75565	3100	37	4105	3994	0.84	0.03	-13.6	-93	15	4063	3448
05-Tibet-54	Apr 05	29.82872	94.74122	3090	34	4079	4057	0.75	0.04	-13.8	-97	13	4110	3512
05-Tibet-55	Apr 05	29.81662	94.74183	3113	3	3688	3677	0.86	0.04	-14.0	-97	15	4156	3576
05-Tibet-56	Apr 05	29.76655	94.73938	3318	81	4311	4263	0.65	0.04	-13.6	-93	16	4072	3460
05-Tibet-57	Apr 05	29.66858	94.71385	3679	9	4381	4346	0.71	0.02	-11.0	-77	11	3279	2539
05-Tibet-58	Apr 05	29.64185	94.69700	3991	10	4494	4484	0.33	0.02	-11.0	-77	12	3307	2567
<i>Lower Yarlung Tsangpo Basin Tributaries</i>														
05Tibet-63	Apr 05	29.43187	94.53787	2940	22	4038	3970	0.26	0.03	-13.2	-95	10	3948	3297
05Tibet-63a	May 04	29.43775	94.54467	2949	11	3760	3704	0.29	0.04	-12.7	-85	16	3820	3137
04Tibet-67	Apr 05	29.61623	94.94100	2901	20	4677	5037	0.82	0.13	-14.7	-108	10	4320	3815
04Tibet-68	Apr 05	29.60640	94.94100	2912	33	4810	5183	0.61	0.14	-14.8	-107	11	4356	3870
05Tibet-69	Apr 05	29.60130	94.93742	2869	54	4486	4445	0.26	0.04	-14.3	-106	8	4230	3682
05-Tibet-70	Apr 05	29.54493	94.89252	3130	0	3400	3173	1.33	0.09	-13.1	-97	8	3937	3282
05-Tibet-71	Apr 05	29.52540	94.88975	3003	0	3720	3050	1.44	0.14	-12.3	-82	16	3694	2986
05Tibet-72	Apr 05	29.51452	94.88097	2935	38	4163	4179	0.32	0.05	-11.9	-80	15	3570	2845
04Tibet-72a	May 04	29.52031	94.88169	2928	6	3605	3587	0.34	0.04	-13.6	-97	12	4070	3457
05Tibet-73	Apr 05	29.46110	94.82880	2941	12	3979	3965	0.30	0.06	-12.5	-85	15	3761	3065

Table 1 (continued)

Sample	Date sampled	Latitude	Longitude	Sample elevation (m)	Drainage area (km ²)	Basin Mean elevation (m)	Precipitation-weighted elevation (m)	Summer (MJJASO) rainfall (m/yr)	Winter (NDJFMA) rainfall (m/yr)	$\delta^{18}\text{O}$	δD	D-excess	Predicted hypsometric elevation ^a	Predicted hypsometric elevation ^b
<i>Lower Yarlung Tsangpo Basin Tributaries</i>														
05Tibet-74	Apr 05	29.44117	94.83260	2954	52	4247	4370	0.39	0.07	-12.6	-86	15	3790	3100
05Tibet-75	Apr 05	29.46265	94.65020	2946	0	4315	2950	0.60	0.05	-12.4	-86	13	3736	3036
NB-8A	May 04	29.50247	94.84256	3124	0	3564	3658	1.06	0.10	-13.5	-93	16	4042	3420
NB-15	May 04	29.44272	94.72583	2962	93	4100	4092	0.29	0.04	-11.4	-74	17	3413	2676
NB-16	May 04	29.44303	94.70425	2938	0	3020	3018	0.53	0.11	-11.6	-90	2	3477	2744
NB-17	May 04	29.45094	94.69356	2951	80	4196	4153	0.36	0.04	-12.9	-88	15	3875	3204
NB-19A	May 04	29.46483	94.61028	2956	0	3663	3208	0.73	0.06	-13.6	-96	13	4072	3460
<i>Middle Yarlung Tsangpo Basin Tributaries</i>														
05Tibet-65	Apr 05	29.34358	94.41618	2955	208	4037	4049	0.23	0.03	-11.6	-80	12	3480	2747
04Tibet-66	Apr 05	29.30765	94.34723	2954	0	2969	2969	0.65	0.03	-11.2	-75	15	3359	2621
05Tibet-76	Apr 05	29.45725	94.81572	2940	19	4093	4142	0.30	0.05	-13.0	-90	14	3913	3252
05Tibet-77	Apr 05	29.23940	94.24772	2940	89	3935	3965	0.31	0.03	-10.4	-68	16	3090	2356
05Tibet-78	Apr 05	29.18588	94.19125	2942	628	3880	3762	0.58	0.03	-9.8	-59	19	2837	2127
05Tibet-79	Apr 05	29.19080	94.12758	2981	27	4181	4127	0.20	0.03	-12.0	-78	18	3602	2881
05Tibet-80	Apr 05	29.18958	94.05875	2974	139	4270	4136	0.22	0.02	-13.4	-91	17	4021	3392
05Tibet-81	Apr 05	29.18485	93.95228	2970	61	4414	4304	0.34	0.03	-13.9	-98	13	4137	3549
05Tibet-82	Apr 05	29.11845	93.86965	2960	1577	4362	4349	0.23	0.02	-12.4	-86	13	3724	3021
05Tibet-84	Apr 05	29.11578	93.81028	2975	47	4368	4366	0.22	0.02	-13.6	-100	9	4057	3439
05Tibet-85	Apr 05	29.12508	93.74030	2994	7	3680	3640	0.35	0.03	-14.7	-107	11	4326	3825
05Tibet-86	Apr 05	29.14830	93.63348	2997	122	4643	4503	0.21	0.01	-15.1	-111	10	4423	3976
05Tibet-87	Apr 05	29.10402	93.44538	3033	101	4591	4595	0.27	0.05	-15.4	-115	8	4491	4084
05Tibet-89	Apr 05	28.99960	93.32063	3038	961	4620	4543	0.22	0.02	-13.9	-101	10	4145	3560
05Tibet-90	Apr 05	28.99870	93.23370	3061	66	4786	4693	0.25	0.04	-15.2	-109	12	4430	3985
05Tibet-91	Apr 05	29.01277	93.16513	3056	48	4485	4399	0.31	0.03	-15.6	-117	8	4519	4131
05Tibet-92	Apr 05	29.04420	93.07642	3101	629	4542	4445	0.28	0.02	-14.4	-107	9	4269	3740
05Tibet-93	Apr 05	29.04483	92.99938	3102	77	4316	4229	0.41	0.01	-15.5	-120	4	4503	4105
05Tibet-95	Apr 05	29.06333	92.82507	3143	710	4547	4482	0.47	0.01	-15.7	-123	2	4535	4158
05Tibet-96	Apr 05	29.07638	92.72213	3161	134	4290	4234	0.58	0.02	-15.9	-124	4	4587	4247
05Tibet-97	Apr 05	29.14055	92.56127	3265	562	4413	4367	0.66	0.02	-16.0	-126	2	4597	4264
05Tibet-98	Apr 05	29.14092	92.51860	3287	348	4384	4316	0.61	0.03	-15.9	-120	7	4584	4242
05Tibet-99	Apr 05	29.04297	92.26315	4081	74	4923	4945	0.44	0.01	-17.3	-134	4	4848	4724
05Tibet-100	Apr 05	29.21933	92.01442	3552	1959	4697	4717	0.41	0.01	-17.2	-137	1	4825	4679
05Tibet-101	Apr 05	29.27865	92.02648	3592	271	4888	4884	0.34	0.01	-17.2	-127	11	4829	4687
05Tibet-103	Apr 05	29.13518	91.79493	3634	1085	4711	4711	0.38	0.01	-17.0	-135	1	4792	4616
<i>Upper Yarlung Tsangpo Tributaries</i>														
W-2-2	Aug 05	29.32663	88.40750	3905	27	4737	4693	0.38	0.00	-19.8	-155	4	5246	5581
W-2-3	Aug 05	29.39653	88.25695	3979	69	4756	4641	0.38	0.00	-20.1	-158	3	5288	5681
W-2-4	Aug 05	29.11387	87.66965	3997	1479	4810	4839	0.27	0.00	-20.4	-161	2	5333	5788
W-2-6	Sept 05	31.53417	79.98182	4490	78	5181	5164	0.10	0.00	-16.2	-120	10	4644	4346
W-2-7	Sept 05	31.45322	80.14172	4762	23	5162	5185	0.17	0.00	-18.2	-140	5	4997	5026
W-2-9	Sept 05	31.05785	81.04598	4765	147	5454	5459	0.17	0.00	-17.1	-127	10	4812	4655
W-2-10	Sept 05	30.95772	81.27500	4624	256	5444	5537	0.40	0.09	-16.5	-120	12	4703	4451
W-2-11	Sept 05	30.69033	81.82975	4749	239	5251	5183	0.11	0.00	-17.4	-130	9	4862	4751
W-2-12	Sept 05	29.77570	83.91422	4606	3	4798	4793	0.24	0.00	-18.4	-147	0	5030	5096
W-2-13	Sept 05	29.54332	84.61832	4607	662	5178	5288	0.21	0.00	-19.9	-156	4	5270	5637
W-2-14	Sept 05	29.42718	85.23408	4706	581	5288	5274	0.23	0.00	-19.6	-156	0	5219	5518
W-2-15	Sept 05	29.33465	85.40513	4528	23	5201	5258	0.26	0.00	-20.5	-155	9	5351	5834
W-2-16	Sept 05	29.37822	85.49460	4636	29	5294	5297	0.26	0.00	-20.1	-156	4	5289	5682
W-2-17	Sept 05	29.50607	86.34075	4741	5	5075	5065	0.20	0.00	-20.8	-165	2	5392	5936
W-2-18	Sept 05	29.36040	86.89668	4571	26	4721	4716	0.34	0.00	-18.9	-153	-2	5117	5285
W-2-19	Sept 05	29.31257	87.03850	4502	4	4705	4702	0.29	0.00	-19.8	-162	-3	5251	5593
W-2-20	Sept 05	29.10472	87.59877	4063	12	4639	4614	0.33	0.01	-19.7	-155	2	5228	5538
W-2-21	Sept 05	29.34287	87.93393	3995	36	4655	4654	0.47	0.00	-19.9	-156	3	5267	5630
W-2-22	Sept 05	29.36852	88.82268	3865	325	5029	4995	0.34	0.00	-19.8	-154	4	5255	5601
W-2-23C	Sept 05	29.32765	89.39650	3805	136	5079	3830	0.35	0.01	-18.5	-148	0	5047	5133
W-2-25	Sept 05	29.33442	90.28042	3742	163	4930	4995	0.31	0.00	-19.7	-156	1	5227	5536
W-2-5	Sept 05	29.31257	87.03850	4502	-	-	-	-	-	-19.8	-160	-2	5241	5569
SUTLEJ	Sept 05	31.47872	79.74468	3669	81	4113	4087	0.099	0.004	-16.3	-122	8	4658	4370
<i>Siang Tsangpo/Brahmaputra Tributaries</i>														
WA-1	Feb 06	28.23653	94.95150	395	5797	2184	1934	1.63	0.16	-6.2	-39	11	1072	887
WA-2	Feb 06	28.28800	94.94693	265	4	867	866	1.17	0.17	-6.8	-40	15	1438	1106
WA-3	Feb 06	28.34967	94.99918	340	9	1303	1301	1.78	0.46	-6.6	-37	15	1318	1032
WA-4	Feb 06	28.59253	95.06933	326	8	1114	1110	1.57	0.58	-5.8	-35	11	833	752
WA-5	Feb 06	28.62243	95.03593	325	14	1361	1355	1.95	0.48	-6.3	-33	17	1154	935
WA-6	Feb 06	28.51203	95.09927	489	1	936	935	1.45	0.60	-6.5	-37	15	1293	1017
WA-7	Feb 06	28.43613	95.10073	411	9	1287	1296	1.63	0.41	-6.7	-40	13	1391	1076
WA-8	Feb 06	28.40302	95.07975	279	57	1237	1242	1.73	0.33	-6.4	-37	14	1230	979
WA-9	Feb 06	28.37528	95.07428	278	1	758	755	1.75	0.37	-6.5	-37	15	1248	990
WA-11	Feb 06	28.35477	95.04078	291	8	997	1003	1.97	0.48	-5.8	-33	13	817	743

(continued on next page)

Table 1 (continued)

Sample	Date sampled	Latitude	Longitude	Sample elevation (m)	Drainage area (km ²)	Basin Mean elevation (m)	Precipitation-weighted elevation (m)	Summer rainfall (MJJASO) (m/yr)	Winter rainfall (NDJFMA) (m/yr)	$\delta^{18}\text{O}$	δD	D-excess	Predicted hypsometric elevation ^a	Predicted hypsometric elevation ^b
<i>Siang Tsangpo/Brahmaputra Tributaries</i>														
WA-12	Feb 06	28.67303	94.96440	329	141	1507	1505	2.52	0.56	-6.8	-37	17	1413	1090
WA-13	Feb 06	28.77693	94.76818	520	140	1657	1666	2.87	0.37	-7.9	-49	15	2030	1496
WA-14	Feb 06	28.73052	94.92362	515	14	1200	1191	2.28	0.53	-6.0	-34	15	993	842
WA-15	Feb 06	28.52598	95.04918	482	66	1621	1622	1.66	0.38	-7.2	-42	15	1639	1232
WA-16	Feb 06	28.30222	95.20203	612	17	1596	1624	2.17	0.44	-7.2	-41	17	1678	1258
WA-17	Feb 06	28.14052	95.09302	259	8	958	960	1.88	0.47	-6.7	-39	15	1367	1062
<i>Southern Tibetan Plateau</i>														
WT06-1	Sept 06	30.54942	91.06520	4562	49	5284	5194	0.32	0.00	-18.0	-130	14	4968	4966
WT06-2	Sept 06	30.51627	91.01683	4566	79	5388	5344	0.33	0.00	-18.1	-136	10	4990	5012
WT06-3	Sept 06	29.93978	90.26558	4632	170	5477	5462	0.37	0.01	-19.0	-140	12	5128	5310
WT06-4	Sept 06	30.07318	90.32860	4800	79	5619	5518	0.27	0.00	-18.5	-141	7	5051	5141
WT06-5	Sept 06	30.14923	90.48977	4531	259	5628	5546	0.37	0.00	-18.5	-140	8	5049	5136
WT06-6	Sept 06	30.30715	90.63402	4926	68	5765	5720	0.35	0.01	-18.5	-139	10	5057	5154
WT06-7	Sept 06	30.35635	90.72327	4652	136	5663	5505	0.61	0.04	-18.2	-131	15	4999	5031
T99-14	May99	30.83010	91.06377	4738	385	5026	5037	0.15	0.02	-17.2	-131	6	4825	4680
T99-15	May99	30.67120	91.09677	5021	2	5280	5514	0.14	0.02	-16.8	-121	13	4756	4549
T99-16	May99	30.60575	91.10977	4841	91	4816	5399	0.14	0.02	-16.8	-123	11	4759	4554
T99-17	May99	30.26393	90.67107	4684	29	5235	4902	0.17	0.02	-15.7	-114	12	4544	4173
T99-18	May99	29.83392	90.74703	3911	97	5682	5252	0.16	0.02	-16.3	-122	9	4672	4394
<i>Central Tibetan Plateau</i>														
WT06-8	Sept 06	32.69820	91.87725	4981	—	—	—	—	—	-12.5	-95	5	3761	3065
WT06-9	Sept 06	32.83052	91.91528	5128	—	—	—	—	—	-17.1	-121	15	4805	4642
WT06-10	Sept 06	33.00825	91.97298	5032	—	—	—	—	—	-15.2	-108	14	4443	4007
T99-1	May99	34.32347	89.00242	4974	481	5310	5303	0.12	0.01	-13.0	-96	8	3918	3258
T99-10	May99	33.00725	88.55177	5105	1	5261	5261	0.14	0.01	-14.3	-108	7	4239	3695
T99-11	May99	31.82112	87.52370	4592	154	4945	4917	0.06	0.01	-15.5	-127	-3	4498	4096
T99-12	May99	31.37042	90.59522	4648	73	4866	4859	0.12	0.01	-15.5	-124	0	4494	4090
T99-13	May99	31.14988	90.75600	4702	514	5221	4910	0.11	0.02	-14.6	-124	-7	4307	3796
T99-2	May99	34.36487	88.87538	4945	434	5252	5242	0.12	0.01	-11.4	-88	3	3435	2699
T99-3	May99	34.25217	88.93108	4982	32	5306	5268	0.12	0.01	-12.3	-93	5	3713	3009
T99-4	May99	34.15945	88.90783	5105	0	5177	5312	0.11	0.01	-11.4	-88	3	3430	2694
T99-5	May99	33.88235	88.86762	5166	468	5202	5177	0.13	0.01	-11.0	-83	5	3284	2544
T99-6	May99	33.61727	88.76107	5004	8	5297	5186	0.14	0.01	-13.3	-97	10	3986	3345
T99-7	May99	33.37698	88.00467	4982	6	5082	5296	0.11	0.01	-11.9	-84	11	3571	2847
T99-8	May99	33.05398	88.69075	4868	12	5206	5154	0.14	0.01	-14.0	-101	11	4153	3572
T99-9	May99	33.02923	88.66833	4930	1	5298	5206	0.12	0.01	-12.2	-85	12	3680	2970
TP 1	Aug 98	33.19093	88.83635	4944	19	5463	5298	0.12	0.01	-11.3	-77	13	3382	2644
TS 1	Aug 98	34.02230	88.88098	5232	3	5566	5487	0.14	0.01	-11.5	-84	8	3446	2711
TS 10	Aug 98	33.39775	88.79517	5080	94	5351	5579	0.15	0.01	-10.5	-68	16	3121	2385
TS 11	Aug 98	33.05670	88.63355	5155	30	5505	5356	0.14	0.01	-12.0	-80	16	3602	2881
TS 12	Aug 98	33.17190	88.81138	4922	56	5501	5529	0.14	0.01	-11.0	-74	14	3304	2565
TS 13	Aug 98	33.13740	88.76797	4930	3	5018	5514	0.15	0.01	-11.1	-73	16	3320	2581
TS 14	Aug 98	33.09175	88.73273	4882	56	5502	5037	0.14	0.01	-10.7	-73	12	3179	2440
TS 15	Aug 98	33.09080	88.73157	4884	6	5349	5514	0.15	0.01	-11.3	-76	14	3396	2658
TS 16	Aug 98	33.05397	88.69073	4876	0	4915	5399	0.14	0.01	-9.5	-74	2	2736	2040
TS 17	Aug 98	33.02918	88.66833	4887	76	5269	4902	0.08	0.01	-12.3	-84	14	3702	2995
TS 18	Aug 98	32.97913	88.45752	4924	153	5163	5252	0.14	0.01	-11.4	-84	8	3440	2705
TS 19	Aug 98	32.69773	88.15475	4915	199	5189	5158	0.08	0.01	-10.0	-72	8	2929	2208
TS 20	Aug 98	32.67652	88.11492	4909	70	5129	5125	0.12	0.01	-11.9	-90	5	3583	2859
TS 21	Aug 98	32.47058	88.06985	4776	18	5182	5264	0.08	0.01	-12.3	-84	14	3697	2990
TS 22	Aug 98	33.56218	88.00403	5205	8	5209	5207	0.11	0.01	-13.2	-90	16	3957	3308
TS 24	Aug 98	32.01908	88.41105	4696	4	4757	4759	0.07	0.01	-13.0	-92	12	3907	3244
TS 25	Aug 98	32.37317	87.99835	4732	58	5294	5341	0.11	0.01	-13.5	-96	12	4031	3405
TS 26	Aug 98	32.32233	87.95678	4712	29	5252	5287	0.10	0.01	-12.8	-95	8	3861	3186
TS 27	Aug 98	32.28248	87.90830	4729	157	5372	5421	0.09	0.01	-12.5	-87	13	3778	3085
TS 3	Aug 98	34.02460	88.89963	5253	42	5580	5573	0.14	0.01	—	-84	—	—	—
TS 4	Jul 98	33.04445	88.63872	5060	36	5619	5616	0.14	0.01	-12.5	-86	14	3761	3066
TS 5	Jul 98	33.05202	88.62600	5000	—	—	—	—	—	—	-103	—	—	—
TS 6	Aug 98	33.28092	88.84390	4955	0	4979	4979	0.14	0.01	-10.3	-66	16	3030	2300
TS 7	Aug 98	33.28530	88.84352	4992	38	5470	5511	0.14	0.01	—	-66	—	—	—
TS 8	Aug 98	33.30093	88.84612	5015	21	5543	5589	0.14	0.01	—	-67	—	—	—
TS 9	Aug 98	33.31870	88.84550	5005	15	5420	5450	0.14	0.01	-11.0	-73	15	3291	2551
<i>Lake Waters</i>														
TL 1	July 98	33.91102	88.59415	5081	12	5000	4995	0.14	0.01	-4.0	-43	-10	-390	141
TL 2	July 98	33.24315	88.83942	4955	93	5065	5041	0.14	0.01	-4.1	-46	-13	-299	183

^a Predicted elevation using $\Delta^{18}\text{O}$ with sea-level $\delta^{18}\text{O} = -3.6\text{‰}$ and thermodynamic model for the isotopic lapse.

^b Predicted elevation using $\Delta^{18}\text{O}$ with sea-level $\delta^{18}\text{O} = -3.6\text{‰}$ and an empirical $2.9\text{‰}/\text{km}$ $\delta^{18}\text{O}$ lapse rate.

Table 2

Slopes and intercepts of local meteoric water lines.

Sample region	No. samples	Slope	Intercept
Nyang Tsangpo	31	8.64	22.0
Po Tsangpo	21	8.48	20.0
L. Yarlung	16	8.83	23.3
M. Yarlung	25	10.05	39.0
U. Yarlung	22	9.76	37.3
Siang Tsangpo	17	6.42	4.3
S. Tibetan Plateau	11	8.144	13.1
C. Tibetan Plateau	44	7.33	0.9

Appendix B. Supplementary data

Supplementary data associated with this article can be found, in the online version, at [doi:10.1016/j.epsl.2009.08.041](https://doi.org/10.1016/j.epsl.2009.08.041).

References

- Aizen, V., Aizen, H., Melack, J., Martma, T., 1996. Isotopic measurements of precipitation on central Asian glaciers (southeastern Tibet, northern Himalayas, central Tian Shan). *J. Geophys. Res.* 101, 9185–9196.
- Anders, A.M., Roe, G.H., Hallet, B., Montgomery, D.R., Finnegan, N.J., Putkonen, J., 2006. Spatial patterns of precipitation and topography in the Himalaya. *Geol. Soc. Am. Spec. Pap.* 398, 39–53.
- Araguás-Araguás, L., Froehlich, K., Rozanski, K., 1998. Stable isotope composition of precipitation over Southeast Asia. *J. Geophys. Res.* 103, 28721–28742.
- Blisniuk, P.M., Stern, L.A., 2005. Stable isotope paleoaltimetry: a critical review. *Am. J. Sci.* 305, 1033–1074.
- Bookhagen, B., Burbank, D.W., 2006. Topography, relief, and TRMM-derived rainfall variations along the Himalaya. *Geophys. Res. Lett.* 33, 1–5.
- Bookhagen, B., Thiede, R.C., Strecker, M.R., 2005. Abnormal monsoon years and their control on erosion and sediment flux in the high, arid northwest Himalaya. *Earth Planet. Sci. Lett.* 231, 131–146.
- Bowen, G.J., Revenaugh, J., 2003. Interpolating the isotopic composition of modern meteoric precipitation. *Water Resour. Res.* 39 (10). [doi:10.1029/2003WR002086](https://doi.org/10.1029/2003WR002086).
- Clark, I., Fritz, P., 1997. Environmental isotopes in hydrogeology. Lewis Publishers, Boca Raton. 328 pp.
- Clemens, S., Prell, W., Murray, D., Shimmield, G., Weedon, G., 1991. Forcing mechanisms of the Indian-Ocean monsoon. *Nature* 353, 720–725.
- Craig, H., 1961. Isotope variations in meteoric waters. *Science* 133, 1702–1703.
- Dansgaard, W., 1964. Stable isotopes in precipitation. *Tellus* 16, 436–468.
- DeCelles, P.G., Quade, J., Kapp, P., Fan, M., Dettman, D.L., Ding, L., 2007. High and dry in central Tibet during the Late Oligocene. *Earth Planet. Sci. Lett.* 253, 389–401.
- Dimri, A., 2006. Surface and upper air fields during extreme winter precipitation over the Western Himalayas. *Pure Appl. Geophys.* 163 (8), 1679–1698.
- Domroes, M., Peng, G., 1988. The climate of China. Berlin, Springer. 361 pp.
- Epstein, S., Mayeda, T.K., 1953. Variations of the $^{18}\text{O}/^{16}\text{O}$ ratio in natural waters. *Geochim. Cosmochim. Acta* 4, 213.
- Friedman, I., Redfield, A.C., Schoen, B., Harris, J., 1964. The variation of the deuterium content of natural waters in the hydrologic cycle. *Rev. Geophys.* 2, 1–124.
- Fritz, P., 1981. River waters. In: Gat, J.R., Gonfiantini, R. (Eds.), *Stable Isotopic Hydrology: Deuterium and Oxygen-18 in the water cycle: IAEA Technical Report*, vol. 210, pp. 177–201.
- Gadgil, S., 2003. The Indian monsoon and its variability. *Annu. Rev. Earth Planet. Sci.* 31, 429–467.
- Garzzone, C.N., Quade, J., DeCelles, P.G., English, N.B., 2000a. Predicting paleoelevation of Tibet and the Himalaya from $\delta^{18}\text{O}$ vs. altitude gradients in meteoric water across the Nepal Himalaya. *Earth Planet. Sci. Lett.* 183, 215–229.
- Garzzone, C.N., Dettman, D.L., Quade, J., DeCelles, P.G., Butler, R.F., 2000b. High times on the Tibetan Plateau: paleoelevation of the Thakkhola graben, Nepal. *Geology* 28, 339–342.
- Garzzone, C.N., Dettman, D.L., Horton, B.K., 2004. Carbonate oxygen isotope paleoaltimetry: evaluating the effect of diagenesis on paleoelevation estimates for the Tibetan Plateau. *Paleogeogr. Paleoclimatol. Paleoecol.* 212, 119–140.
- Gat, J.R., 1996. Oxygen and hydrogen isotopes in the hydrologic cycle. *Annu. Rev. Earth Planet. Sci.* 24, 225–262.
- Gat, J.R., Matsui, E., 1991. Atmospheric water balance in the Amazon Basin: an isotopic evapo-transpiration model. *J. Geophys. Res.* 96, 13179–13188.
- Gonfiantini, R., 1978. Standards for stable isotope measurements in natural compounds. *Nature* 271, 534–536.
- Graham, S.A., Chamberlain, C.P., Yue, Y., Ritts, B., Hanson, A., Horton, T.W., Waldbauer, J.W., Poage, M.A., Feng, X., 2005. Stable isotope records of Cenozoic climate and topography, Tibetan Plateau and Tarim basin. *Am. J. Sci.* 305, 101–118.
- Hren, M.T., Chamberlain, C.P., Hilley, G.E., Blisniuk, P.M., Bookhagen, B., 2007. Major ion chemistry of the Yarlung Tsangpo-Brahmaputra river: chemical weathering, erosion, and CO_2 consumption in the southern Tibetan Plateau and eastern syntaxis of the Himalaya. *Geochim. Cosmochim. Acta* 71, 2907–2935.
- Karim, A., Veizer, J., 2002. Water balance of the Indus River Basin and moisture source in the Karakoram and western Himalayas: Implications from hydrogen and oxygen isotopes in river water. *J. Geophys. Res. Atmos.* 107. [doi:10.1029/2000JD000253](https://doi.org/10.1029/2000JD000253).
- Kendall, C., Coplen, T.B., 2001. Distribution of oxygen-18 and deuterium in river waters across the United States. *Hydrol. Proced.* 15, 1363–1393.
- Kent-Corson, M.L., Ritts, B.D., Zhuang, G., Bovet, P.M., Graham, S.A., Chamberlain, C.P., 2009. Stable isotopic constraints on the tectonic, topographic, and climatic evolution of the northern margin of the Tibetan Plateau. *Earth Planet. Sci. Lett.* 282, 158–166.
- Koster, R.D., Perry, D., Jouzel, J., 1993. Continental water recycling and H_2^{18}O concentrations. *Geophys. Res. Lett.* 20, 2215–2218.
- Lang, T.J., Barros, A.P., 2004. Winter storms in the central Himalayas. *J. Meteorol. Soc. Jpn.* 82 (3), 829–844.
- Liu, Z., Tian, L., Yao, T., Yu, W., 2008a. Seasonal deuterium excess in Nagqu precipitation: influence of moisture transport and recycling in the middle of the Tibetan Plateau. *Environ. Geol.* 55, 1501–1506.
- Liu, Z., Tian, L., Chai, X., Yao, T., 2008b. A model-based determination of spatial variation of precipitation $\delta^{18}\text{O}$ over China. *Chem. Geol.* 249, 203–212.
- Merlivat, L., Jouzel, J., 1979. Global climatic interpretation of the deuterium-oxygen 18 relationship for precipitation. *J. Geophys. Res.* 84, 5029–5033.
- Murphy, M., Saylor, J.E., Ding, L., 2009. Late Miocene topographic inversion in southwest Tibet based on integrated paleoelevation reconstructions and structural history. *Earth Planet. Sci. Lett.* 282, 1–9.
- Pande, K., Pradia, J.T., Ramesh, R., Sharma, K.K., 2000. Stable isotope systematics of surface water bodies in the Himalayan and Trans-Himalayan (Kashmir) region. *Proc. Indian Acad. Sci.* 109–115.
- Poage, M.A., Chamberlain, C.P., 2001. Empirical relationships between elevation and the stable isotope composition of precipitation: considerations for studies of paleoelevation change. *Am. J. Sci.* 301, 1–15.
- Quade, J., Garzzone, C., Eiler, J., 2007. Paleoelevation reconstruction using pedogenic carbonates. *Rev. Mineral.* 66, 53–87.
- Reiser, A.B., Bojar, A.V., Neubauer, F., Genser, J., Liu, Y., Ge, X.H., Friedl, G., 2008. Monitoring Cenozoic climate evolution of northeastern Tibet: stable isotope constraints from the western Qaidam Basin, China. *Int. J. Earth Sci.* [doi:10.1007/s00531-008-0304-5](https://doi.org/10.1007/s00531-008-0304-5).
- Rowley, D.B., 2007. Stable isotope-based paleoaltimetry: theory and validation. *Rev. Mineral. Geochem.* 66, 23–52.
- Rowley, D.B., Currie, B.S., 2006. Palaeo-altimetry of the late Eocene to Miocene Lunpola basin, central Tibet. *Nature* 439, 677–681.
- Rowley, D.B., Garzzone, C., 2007. Stable isotope-based paleoaltimetry. *Annu. Rev. Earth Planet. Sci.* 35, 463–508.
- Rowley, D.B., Pierrehumbert, R.T., Currie, B.S., 2001. A new approach to stable isotope-based paleoaltimetry: implications for paleoaltimetry and paleohypsometry of the High Himalaya since the Late Miocene. *Earth Planet. Sci. Lett.* 188, 253–268.
- Rozanski, K., Araguás-Araguás, L., Gonfiantini, R., 1993. Climate change in continental isotopic records 1–36. American Geophysical Union, Washington.
- Saylor, J.E., Quade, J., Dettman, D.L., DeCelles, P.G., Kapp, P.A., Ding, L., 2009. The late Miocene through present paleoelevation history of southwestern Tibet. *Am. J. Sci.* 309, 1–42. [doi:10.2475/01.2009.01](https://doi.org/10.2475/01.2009.01).
- Siegenthaler, U., Oeschger, H., 1980. Correlation of ^{18}O in precipitation with temperature and altitude. *Nature* 285, 314–317.
- Thompson, L.G., Yao, T., Mosley-Thompson, E., Davis, M.E., Henderson, K.A., Lin, P.N., 2000. A high-resolution millennial record of the South Asian monsoon from Himalayan ice cores. *Science* 289, 1916–1919.
- Tian, L., Yao, T., Numaguti, A., Sun, W., 2001a. Stable isotope variations in monsoon precipitation on the Tibetan Plateau. *J. Meteorol. Soc. Jpn.* 79, 959–966.
- Tian, L., Masson-Delmotte, V., Stievenard, M., Yao, T., Jouzel, J., 2001b. Tibetan Plateau summer monsoon northward extent revealed by measurements of water stable isotopes. *J. Geophys. Res.* 106, 28,081–28,088.
- Tian, L., Yao, T., Numaguti, A., Duan, K., 2001c. Relation between stable isotope in monsoon precipitation in southern Tibetan Plateau and moisture transport history. *Sci. China (D)* 44.
- Tian, L., Yao, T., Schuster, P.F., White, W.C., Ichiyangui, K., Pendall, E., Pu, J., Yu, W., 2003. Oxygen-18 concentrations in recent precipitation and ice cores on the Tibetan Plateau. *J. Geophys. Res.* 108, 4293. [doi:10.1029/2002JD002173](https://doi.org/10.1029/2002JD002173).
- Tian, L., Yao, T., White, J.W.C., Yu, W., Wang, N., 2005. Westerly moisture transport to the middle of Himalayas revealed from the high deuterium excess. *Chin. Sci. Bull.* 50, 1026–1030.
- Tian, L., Yao, T., MacClune, K., White, J.W.C., Schilla, A., Vaughn, B., Vachon, R., Ichiyangui, K., 2007. Stable isotopic variations in west China: a consideration of moisture sources. *J. Geophys. Res.* 112, D10112. [doi:10.1029/2006JD007718](https://doi.org/10.1029/2006JD007718).
- Tian, L., Ma, L., Yu, W., Yin, C., Zhao, Z., Tang, W., Wang, Y., 2008. Seasonal variations of stable isotope in precipitation and moisture transport at Yushu, eastern Tibetan Plateau. *Sci. China (D)* 51, 1121–1128.
- Vennemann, T.W., O'Neil, J.R., 1993. A simple and inexpensive method of hydrogen isotope and water analyses of minerals and rocks based on zinc reagent. *Chem. Geol.* 103, 227–234.
- Vuille, M., Werner, M., Bradley, R.S., Keimig, F., 2005. Stable isotopes in precipitation in the Asian monsoon region. *J. Geophys. Res.* 110. [doi:10.1029/2005JD006022](https://doi.org/10.1029/2005JD006022).
- Wang, Y., Wang, X., Xu, Y., Zhang, C., Li, Q., Tseng, Z.J., 2008. Stable isotopes in fossil mammals, fish, and shells from Kunlun Pass Basin Tibetan Plateau: paleo-climatic and paleo-elevation implications. *Earth Planet. Sci. Lett.* 270, 73–85.
- Wushiki, H., 1981. Some characteristics of stable isotope content in the Himalayan waters. *Geological and Ecological Studies of Qinghai-Xizang Plateau*, pp. 1671–1676.

- Yu, J., Zhang, H., 1981. Oxygen isotopic composition of meteoric water in the eastern part of Xizang. *Geological and Ecological Studies of Qinghai–Xizang Plateau*, pp. 1677–1686.
- Yurtsever, Y., Gat, J., 1981. Atmospheric waters. In: Gat, J.R., Gonfiantini, R. (Eds.), *Stable Isotope Hydrology: Deuterium and Oxygen-18 in the Water Cycle*, pp. 103–142. IAEA, Vienna, Austria.
- Zhang, X., 1997. Variation of $\Delta\delta^{18}\text{O}/\Delta T$ in precipitation in the Qinghai–Xizang Plateau. *Chin. Geogr. Sci.* 7, 339–346.
- Zhang, X., Nakawo, M., Yao, T., Han, J., Xie, Z., 2002. Variations of stable isotopic compositions in precipitation on the Tibetan Plateau and its adjacent regions. *Sci. China (D)*.